



Synthesis of titanium containing MCM-41 and its application for catalytic hydrolysis of cellulose



Dewen He^a, Cancheng Bai^b, Chongwen Jiang^{b,c,*}, Tao Zhou^b

^a College of Metallurgical Science and Engineering, Central South University, Changsha 410083, China

^b College of Chemistry and Chemical Engineering, Central South University, Changsha 410083, China

^c Key laboratory of Resource Chemistry of Nonferrous Metals, Ministry of Education, Central South University, Changsha 410083, China

ARTICLE INFO

Article history:

Received 2 December 2012

Received in revised form 30 June 2013

Accepted 26 July 2013

Available online 2 August 2013

Keywords:

Titanium

MCM-41

Hydrolysis

Cellulose

ABSTRACT

Titanium containing MCM-41 is synthesized hydrothermally in the presence of structure-directing agent cetyltrimethylammonium bromide (CTAB). Bi- and tri-metal Fe and Zn are impregnated in these materials to improve the acid catalytic sites as well. XRD, BET nitrogen adsorption isotherm, TEM and SEM analysis confirm the presence of mesopores in the composite. The local environment of titanium incorporated into the mesoporous silicate material is investigated by FT-IR and UV-Vis spectroscopy. These results indicate the presence of active centers within the composite material Ti, Fe and Zn. The new composite materials are preliminarily tested in the hydrolysis of cellulose. All the titanium MCM-41 materials improve the conversion of cellulose, providing higher catalytic activity in hydrolysis. There is maximum sugar and 5-HMF concentration resulted from hydrolysis of cellulose with Fe/Ti-MCM-41 catalyst.

Crown Copyright © 2013 Published by Elsevier B.V. All rights reserved.

1. Introduction

Mesoporous molecular sieves possess large pore dimensions and narrow pore-size distributions. These materials have been found promising candidates as catalysts, absorbents and supports [1,2]. Of the particular interest is MCM-41 materials which may be used as solid acid catalysts. The catalytic properties of molecular sieves rely on the presence of active sites in their frameworks. In the case of MCM-41, the incorporation of hetero atoms to the otherwise electrically neutral purely siliceous framework may generate active sites, which was found to change considerably the activity of the catalyst with respect to the parent material. A combination of the large pore dimensions of mesoporous materials with the catalytic active sites in these structures would be highly advantageous leading to novel and probably useful catalysts or catalyst carriers [3–6].

Recent studies including metal containing mesoporous materials mostly involve the specific reactions that can take place in hydroxylation and alkylation of phenol, oxidation and dehydrogenation of hydrocarbons, biomass pyrolysis, methanol synthesis and photo-catalysis [7–12]. The literatures concerning successful incorporation of metal hetero atoms into MCM-41 materials have been developing. With the incorporation of various metals (Al, Ti, Co, Mo, Fe, Cu), it was found that the catalytic properties of these materials could be improved [13]. The field of mesoporous titanium silicates is one of the fastest developing areas of porous materials. The attempts to obtain titanium materials

with high catalytic activity and tunable catalytic behavior lead to the development of various processes for their synthesis. The impregnation technique usually results in the formation of crystalline TiO₂ nanoparticles located on the external surface of the mesoporous silica matrix. On the contrary, titanium species predominantly in tetrahedral co-ordination could be obtained by hydrothermal direct synthesis, but this procedure restricts the introducible amount of titanium to some extent [14].

Even though the active sites existing in the mesopores of the titanium-containing MCM-41 were investigated earlier by different techniques, many questions have remained open and their chemical strength and nature continues even under discussion. Consequently, for the application of MCM-41 in catalysis, a detailed knowledge concerning the activity sites of these materials is desirable. Up to now most of the literatures in the field of composites have focused on a preparation of new composites with different transitional metals but only a few of them have emphasized on bi- or tri-metallic modified MCM-41 molecular sieves. This paper describes a synthetic procedure that leads to titanium containing Ti-MCM-41 mesoporous materials, which iron and zinc are introduced into mesoporous siliceous matrices by impregnation method. X-ray diffraction (XRD) and nitrogen adsorption isotherm analysis are used to confirm the presence of mesopores in the composite. High resolution transmission electron microscopy (TEM) and scanning electron micrographs (SEM) are used to confirm mesopores at the same area of investigation. FT-IR, UV-Vis spectra and ICP-AES are used to provide the information about the titanium location. Iron and zinc containing Ti-mesoporous materials have been selected for the current study, and their catalytic activity has been evaluated by hydrolysis of cellulose. Our intention is to enhance the knowledge of the relation

* Corresponding author at: College of Chemistry and Chemical Engineering, Central South University, Changsha 410083, China. Tel./fax: +86 731 88879616.

E-mail address: jcwcsu@csu.edu.cn (C. Jiang).

between the formed products and the properties of the catalysts applied. This titanium containing MCM-41 pioneered the potential hydrolysis bulky molecules which cannot enter into the micropores of zeolites.

2. Experimental

2.1. Synthesis of Ti-MCM-41

The synthesis process of Ti-MCM-41 with Si/Ti molar ratio equal to 30 was similar to that of literature [3]. The specific synthesis procedure was as follows. The cetyltrimethylammonium bromide (CTAB, Tianjin Kermel Chemical Reagent Co. Ltd., China) was dissolved in distilled water by stirring at 60 °C. Then the Na_2SiO_3 (Aladdin reagent Co. Ltd., China) was dissolved in distilled water and was dripped into the CTAB solution. This mixture was stirred for 15 min. A certain amount of $\text{Ti}(\text{SO}_4)_2$ (Aladdin reagent Co. Ltd., China) was dissolved in 1 mol/L sulphuric acid and was added into the mixture with stirring. Subsequently, the pH was adjusted rapidly to 9 by sulphuric acid. After stirring at 40 °C for 35 min, the resulting mixture was transferred into a stainless-steel autoclave reactor and heated to 130 °C for 48 h under static conditions. The solid product filtered was washed to neutral with distilled water and dried in air at 90 °C overnight. The as-synthesized sample was calcined at 550 °C in the air for 5 h to remove the template CTAB, and then the desirable Ti-MCM-41 was obtained.

2.2. Synthesis of Fe/Ti-MCM-41, Zn/Ti-MCM-41 and Fe-Zn/Ti-MCM-41

A sufficient amount of ferric nitrate ($\text{Fe}(\text{NO}_3)_3 \cdot 9\text{H}_2\text{O}$) was dissolved in a minimum amount of distilled water and the calcined Ti-MCM-41 was added into the solution. Thereafter, water was added into the mixture to achieve the complete wetting of the solid material. The mixture was kept in an ultrasonic bath for 30 min and then dried at 60 °C for 21 h. The dried product was calcined at 500 °C for 3 h to obtain the Fe/Ti-MCM-41.

Zn/Ti-MCM-41 and Fe-Zn/Ti-MCM-41 were synthesized in the same process. The mass fractions of the loaded metal oxide in the Fe/Ti-MCM-41, Zn/Ti-MCM-41 and Fe-Zn/Ti-MCM-41 were 5%. And the total mass fraction of Fe and Zn oxide in the Fe-Zn/Ti-MCM-41 sample was 10%.

2.3. Methods of characterization

XRD patterns of all samples were recorded on a Rigaku D/max-2500 diffractometer instrument at 50 kV and 200 mA with $\text{Cu K}\alpha$ irradiation. FT-IR spectra was recorded on a FT-IR spectrometer (Nicolet, Avatar360) using the KBr pellet technique by making 32 scans at 4 cm^{-1} resolution. N_2 adsorption-desorption was measured on a Micromeritics Tristar 3000 micropore analysis system. The UV-Vis spectra were obtained on Shimadzu UV-2450 spectrophotometer and the chemical composition in the Fe/Ti-MCM-41, Zn/Ti-MCM-41 and Fe-Zn/Ti-MCM-41 were analyzed using ICP-AES with PerkinElmer Optima 5300 DV. TEM and SEM were obtained on a FEI Tecnai G2 F20 and Quanta-200 scanning electron microscope using conventional sample preparation and imaging techniques, respectively.

The hydrolysis experiments were carried out using a 250 mL high pressure reactor (WHF-0.25 L, Weihai Automatic Control Reaction Kettle Corp., China). Each cellulose sample (Aladdin reagent Co. Ltd., China) mixed with 50 water and 5% (w.%) catalyst was heated to 230 °C, which was the maximum temperature in the closed reactor. The stirrer speed was adjusted to 50 rpm and the reactor temperature was measured using a thermocouple probe connected to the control unit ($\pm 1\text{ }^\circ\text{C}$). The reaction was stopped and cooled to room temperature as soon as possible. After each hydrolysis run, the aqueous was filtered. The filtrates were analyzed using DNS method to determine the total sugar, and 5-Hydroxymethyl furfural (5-HMF) content was analyzed using HP 1100 HPLC with mobile phase of 35% methanol (vol.%) in water, equipped with Dikma ODS column and UV detector (254 nm).

Authentic sample of 5-HMF was used as standard and calibration curves for quantification.

3. Results and discussion

3.1. Physico-chemical characterization of the samples

Fig. 1 shows the various XRD patterns of titanium containing mesoporous materials. All sample presents well-defined (100) reflections in their XRD patterns. These results suggest that the as-synthesized samples are in the structure of MCM-41. However, there are no well resolved peaks (110, 200, 210), which are clearly visible corresponding pure silica analogs, indicating that the samples possess low long-range ordered structures. These (100) reflections moved slightly to the right and concurrently long range order of MCM-41 diminished somewhat as Ti and hetero atom were incorporated. The Ti-MCM-41 molecular sieve has a relative intense (100) peak compared to Ti-MCM-41 samples impregnated with Zn and Fe metal species, which led to a reduction of the low-angle XRD indicative of the meso-character of the porous matrix. This can be caused by either lattice destruction or successful introduction of Zn and Fe metal elements into the pore system [11].

Figs. 2 to 6 presents the N_2 adsorption-desorption and the corresponding pore size distribution curves for Ti-MCM-41 samples. The isotherms of Ti-MCM-41 materials are of type IV, indicating the preservation of the mesoporous structure. The abrupt increase in the p/p_0 from 0.25 to 0.4 means a sharp inflection characteristic of capillary condensation within the mesopores. This prominent swing can be used to relate to the structure of the mesopores, and its position determines the characteristic pore size. The fact that the p/p_0 value of Ti-MCM-41 shifts to a lower value compared to that of MCM-41 suggests that the pore size of Ti-MCM-41 decreases with the introduction of titanium species. The BJH data show approximately 2.4 to 2.7 nm mean pore diameter for titanium containing MCM-41 samples, and this matches well with other distribution curves reported earlier [12,13]. Since titanium species introduced post-synthetically would be expected to react with surface silanol groups of the walls in a random fashion, the pores with largest population would make a contact with titanium species in relatively high probability. As a consequence, the incorporation of titanium, iron and zinc species results in slight reduction in average pore size.

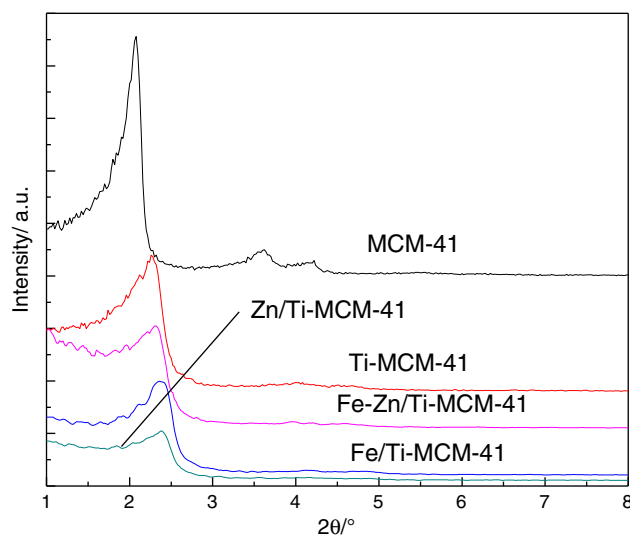


Fig. 1. XRD patterns of MCM-41, non-calcined Ti-MCM-41, Ti-MCM-41, Fe/Ti-MCM-41, Zn/Ti-MCM-41 and Fe-Zn/Ti-MCM-41.

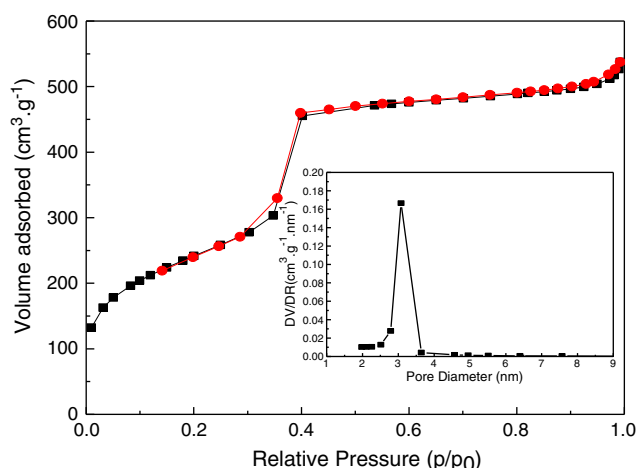


Fig. 2. Nitrogen physisorption isotherms and pore size distribution (inset) for the MCM-41.

The textural properties of all the samples are listed in Table 1. The surface area values decrease for all the Ti-MCM-41 samples compared to the parent MCM-41 materials. This has previously been observed for MCM-41. Moreover, the surface area decreases in order Fe/Ti-MCM-41 > Zn/Ti-MCM-41 > Fe-Zn/Ti-MCM-41 > Ti-MCM-41, which are due to the incorporation of different metals in the materials.

The FT-IR spectra of the titanium incorporated and hydrothermally prepared mesoporous molecular sieves are given in Fig. 7. Two bands at around 1082 and 1228 cm^{-1} associated to internal and external asymmetric Si–O stretching modes as well as two bands (800 and 457 cm^{-1}) assigned to symmetric stretching and tetrahedral bending of Si–O bonds, respectively, can be observed. A strong band at 962 cm^{-1} is clearly visible in the FT-IR spectra of Ti-MCM-41 samples. For Ti-containing zeolites, the band at 960 cm^{-1} is believed to be a consequence of the stretching vibration of Si–O units bound to Ti atoms [15,16]. However, caution is required in assigning this band since pure silica MCM-41 also exhibits such a band around 960 cm^{-1} attributed to the N(Si–OH) vibration of silanol groups at the defect sites present in the mesoporous structure. The 960 cm^{-1} band also occurs in the spectra of Ti-free mesoporous molecular sieves due to the abundance of silanol groups present in the calcined samples and cannot be used as a criterion to claim the incorporation of titanium into the framework

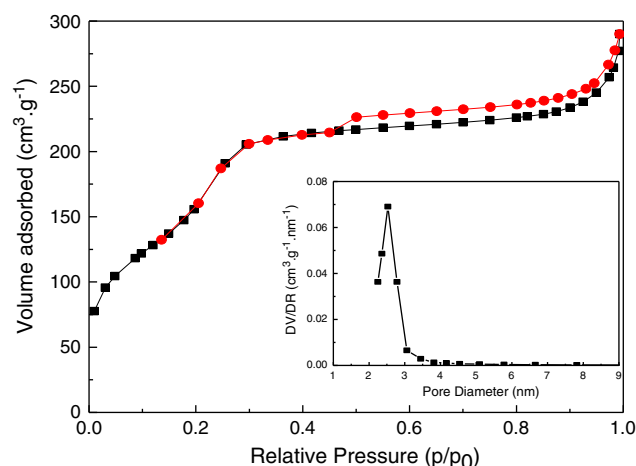


Fig. 4. Nitrogen physisorption isotherms and pore size distribution (inset) for the Fe/Ti-MCM-41.

[17]. Thus, this band can be interpreted in terms of the overlapping of both Si–OH groups and Ti–O–Si bonds vibrations. After impregnation of Fe and Zn in titanium containing MCM-41, additional features can't be observed except for the intensities of the correspond band.

The DR UV-Vis spectra of Ti-MCM-41 in Fig. 8 shows an intense band centered at 210 nm with a weak shoulder band in the range 250–300 nm, and these bands are different from those of pure silica MCM-41, suggesting that framework titanium species dominate in the mesoporous sieves, and the presence of the shoulder band can be caused by some adsorbates remaining in the sample. Furthermore, the UV-Vis spectra of Fe/Ti-MCM-41 exhibits a stronger absorption band in the 210–290 nm region attributable to isolated, tetrahedrally coordinated iron and titanium species, compared with Ti-MCM-41. The bands over 300 nm may arise from the presence of oligomeric FeOx species and finely dispersed Fe₂O₃ nanoparticles.

Table 1 also summarizes the chemical composition analysis of these samples with ICP-AES. However, the practical metal content is less than the theoretical content, resulting from some loss of metal during the synthesis.

TEM images of Ti-MCM41 sample are shown in Fig. 9. The TEM micrographs confirm that the material contain long-range order, one dimensional pore structure, similar to the pure silicon MCM-41 [2].

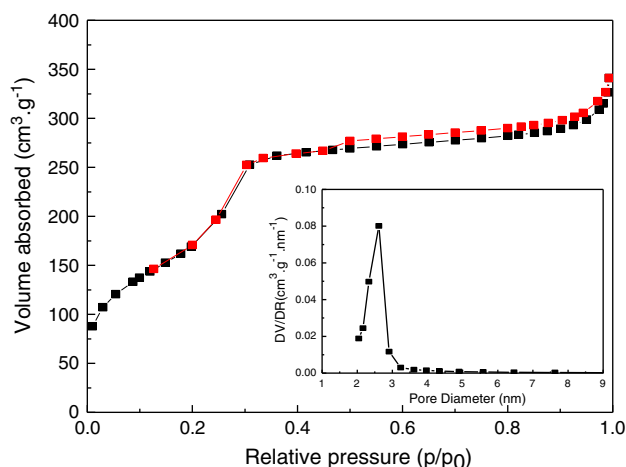


Fig. 3. Nitrogen physisorption isotherms and pore size distribution (inset) for the Ti-MCM-41.

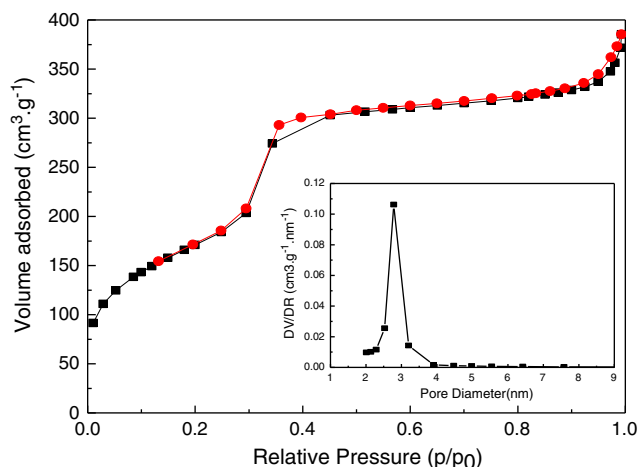


Fig. 5. Nitrogen physisorption isotherms and pore size distribution (inset) for the Zn/Ti-MCM-41.

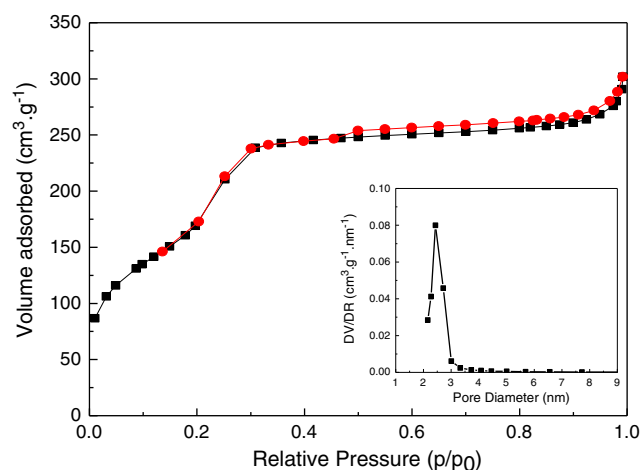


Fig. 6. Nitrogen physisorption isotherms and pore size distribution (inset) for the Fe-Zn/Ti-MCM-41.

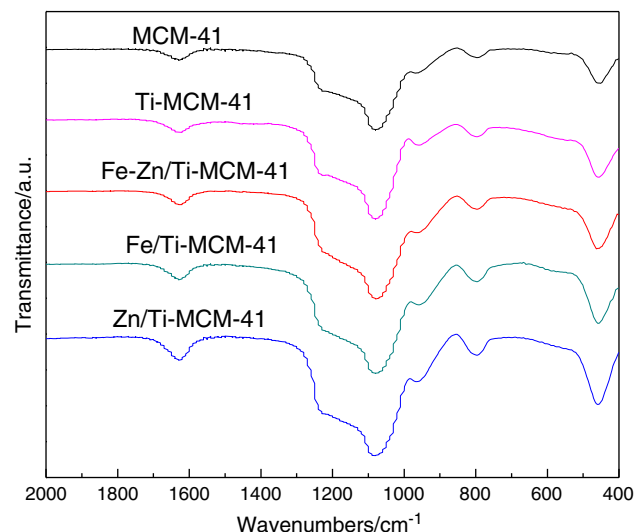


Fig. 7. FT-IR spectra of the initial and the modified samples.

Parallel straight pores and hexagonally arrayed pores can be ascribed to the (110) directions of hexagonal symmetry phase, which is too weak to recognize in XRD. These results, together with the XRD patterns, confirm the formation of low long-range ordered mesostructure. SEM photographs in Fig. 9 show typical morphologies of the particles of all the samples, respectively. The size of the particles is difficult to define because of the tendency of mesoporous molecular sieves to form aggregation. The SEM in Fig. 10 for the titanium containing MCM-41 show the particles are likely spherical in nature and uniformly distributed throughout the surfaces.

3.2. Evaluation of catalytic activity

Five Titanium containing MCM-41 catalysts, including non-calcined Ti-MCM-41, Ti-MCM-41, Zn/Ti-MCM-41, Fe/Ti-MCM-41 and Fe-Zn/Ti-MCM-41, are chosen as catalysts to determine their effects on the hydrolysis of cellulose. In order to easily compare the results of different sort of catalysts, the concentrations of four catalyst used are 5% cellulose weight, and all experiments were conducted under the same operating conditions. Table 2 presents the results of control cellulose during hydrolysis process with hot water only or different titanium containing MCM-41 catalysts. The experimental data suggested that all the titanium containing MCM-41 catalysts but non-calcined Ti-MCM-41 increase the hydrolysis conversion of cellulose in comparison with hot water only. Furthermore, conversion of cellulose with catalysts impregnated Fe and Zn increases more than Ti-MCM-41 only. This means that the addition of Fe and Zn in Ti-MCM-41 can further improve the acid active sites of the catalyst, which facilitates the cellulose hydrolysis. The major components obtained from cellulose are total sugar and 5-HMF, dehydration of 6-carbon sugar.

Table 1
Chemical composition and physicochemical characteristic of the catalysts.

Catalyst	Surface area (m ² /g)	BJH pore diameter (nm)	Total pore volume (g/cm ³)	Ti/Fe/Zn (ICP, wt.%)
MCM-41	864.41	3.85	0.832	–
Ti-MCM-41	776.74	2.72	0.527	0.90/0/0
Used Ti-MCM-41	546.90	2.27	0.316	–
Fe/Ti-MCM-41	686.55	2.60	0.446	0.90/3.4/0
Zn/Ti-MCM-41	690.89	2.48	0.429	0.90/0/3.5
Fe-Zn/Ti-MCM-41	722.39	2.69	0.486	0.90/2.4/2.5

Consequently, the maximum sugar and 5-HMF concentration are obtained with Fe/Ti-MCM-41 catalyst. One possible explanation for this observation is trivalent Fe is more efficient catalyst for the selectivity of sugar and 5-HMF [18]. Moreover, it is observed that the concentrations of sugar with Ti-MCM-41, Zn/Ti-MCM-41 and Fe/Ti-MCM-41 are nearly equal, whereas 5-HMF concentration with Zn/Ti-MCM-41 decreases obviously even less than hot water only. This difference can be inferred that the introduction of Zn leads to reduction to the selectivity of 5-HMF. In contrast, non-calcined Ti-MCM-41 shows low activity in hydrolysis of cellulose. The yield of sugar and 5-HMF catalyzed by non-calcined Ti-MCM-41 are even less than hot water only, probably owing to that the decreased external surface area of non-calcined Ti-MCM-41 is the main contributor to catalytic activity loss to some extent. Hereafter, the stability of the used Ti-MCM-41 sample is also examined by using XRD and nitrogen adsorption/desorption measurements. The XRD peak intensity of used Ti-MCM-41 sample in Fig. 1 decreases more than 70% after catalytic hydrolysis cellulose at 230 °C for 30 min, and the destruction

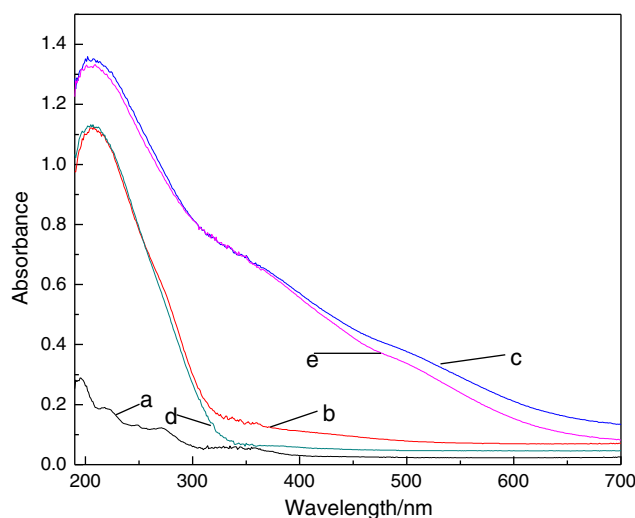


Fig. 8. DR UV–Vis spectra of all the samples: MCM-41 (a), Ti-MCM-41 (b), Fe/Ti-MCM-41 (c), Zn/Ti-MCM-41 (d), Fe-Zn/Ti-MCM-41 (e).

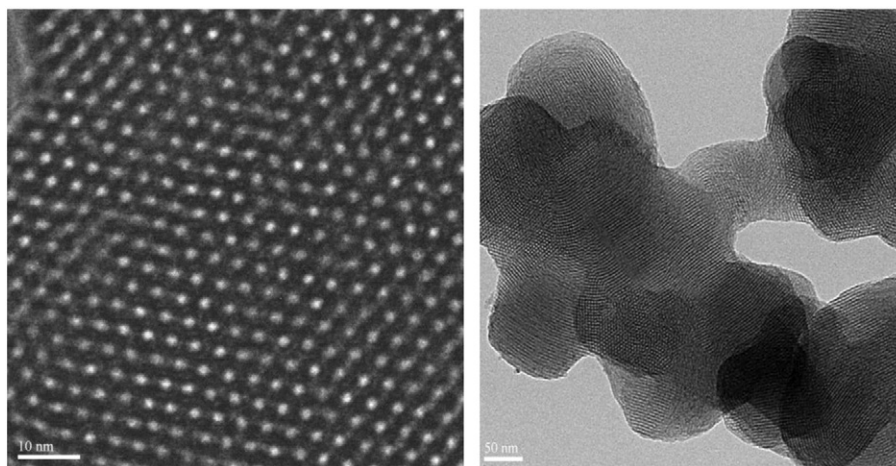


Fig. 9. TEM image of Ti-MCM-41.

of framework is an irreversible process. The nitrogen adsorption/desorption measurements in Fig. 11 shows that the step corresponding to nitrogen condensation in primary mesopores in used Ti-MCM-41 sample is broad, indicating a rather low degree of structure ordering [19]. In addition, the BET surface area, the pore diameter and the pore volume of used Ti-MCM-41 samples after catalytic hydrolysis obviously decrease, respectively. These facts indicate that the poor stability of Ti-MCM-41 due to loss of mesoporous structure may cause unfavorable effect when it is reused to catalytic hydrolysis of cellulose.

4. Conclusions

Five titanium containing mesoporous materials non-calcined Ti-MCM-41, Ti-MCM-41, Fe/Ti-MCM-41, Zn/Ti-MCM-41 and Fe-Zn/Ti-MCM-41 were synthesized and characterized. And all the samples show XRD, FT-IR and BET patterns typical of MCM-41. The metallic modified mesoporous silica materials have strong influences on the state of the incorporated titanium species and its catalytic properties. In contrast to the hot water only, all the titanium MCM-41 materials improve the conversion of cellulose, providing higher catalytic activity in hydrolysis.

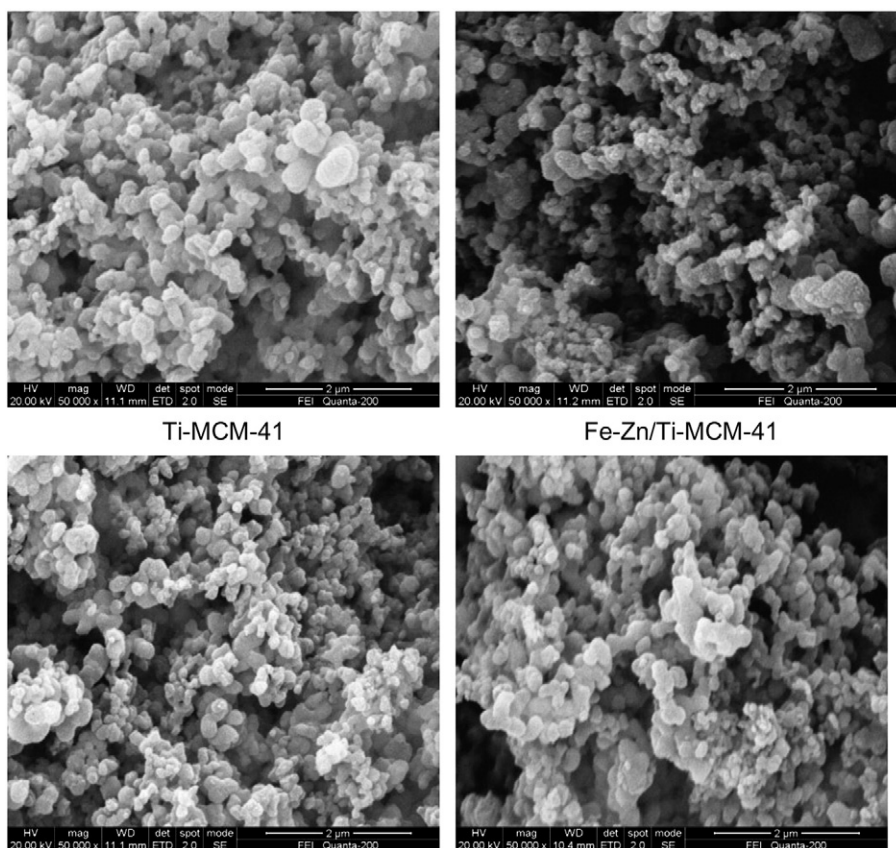


Fig. 10. SEM images of Ti-MCM-41, Fe/Ti-MCM-41, Zn/Ti-MCM-41 and Fe-Zn/Ti-MCM-41.

Table 2
Evaluation of titanium MCM-41 catalyst in hydrolysis of cellulose.

Catalyst	Conversion (%)	Total sugar (g/L)	5-HMF (g/L)
Hot water only	32.01	2.06	1.49
Non-calcined Ti-MCM-41	32.79	1.98	1.36
Ti-MCM-41	35.57	2.42	1.96
Fe-Zn/Ti-MCM-41	46.53	2.34	1.85
Zn/Ti-MCM-41	46.22	2.41	1.19
Fe/Ti-MCM-41	44.96	3.09	2.29

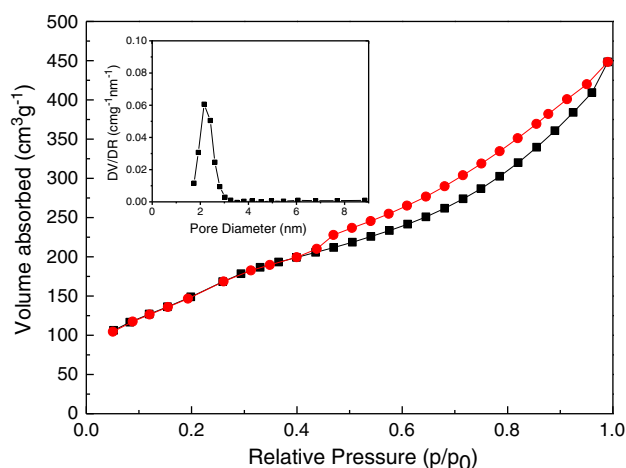


Fig. 11. Nitrogen physisorption isotherms and pore size distribution (inset) for the used Ti-MCM-41.

The maximum sugar and 5-HMF concentration are obtained with Fe/Ti-MCM-41 catalyst.

Acknowledgments

The authors thank China–Japan International Cooperation Project (2010DFA41440) and Creative Project of Hunan Province Science & Technology Office of China (2010XK6003) for supporting this work.

References

- [1] C.T. Kresge, M.E. Leonowicz, W.J. Roth, J.C. Vartuli, J.S. Beck, Ordered mesoporous molecular sieves synthesized by a liquid-crystal template mechanism, *Nature* 359 (1992) 710–712.
- [2] P. Selvam, S.K. Bhatia, C.G. Sonwane, Recent advances in processing and characterization of periodic mesoporous MCM-41 silicate molecular sieves, *Ind. Eng. Chem. Res.* 40 (2001) 3237–3261.
- [3] F.S. Xiao, Y. Han, Y. Yu, X.J. Meng, M. Yang, S. Wu, Hydrothermally stable ordered mesoporous titanasilicates with highly active catalytic sites, *J. Am. Chem. Soc.* 124 (2006) 888–889.
- [4] O.A. Anunziata, M.L. Martínez, M.G. Costa, Characterization and acidic properties of Al-SBA-3 mesoporous material, *Mater. Lett.* 64 (2010) 545–548.
- [5] M.H. Nilsen, E. Antonakou, A. Bouzga, A. Lappas, K. Mathisen, M. Stöcker, Investigation of the effect of metal sites in Me–Al-MCM-41 (Me = Fe, Cu or Zn) on the catalytic behavior during the pyrolysis of wooden based biomass, *Microporous Mesoporous Mater.* 105 (2007) 189–203.
- [6] M.M.L. Ribeiro Carrott, F.L. Conceição, J.M. Lopes, P.J.M. Carrott, C. Bernardes, J. Rocha, F. Ramôa Ribeiro, Comparative study of Al-MCM materials prepared at room temperature with different aluminum sources and by some hydrothermal methods, *Microporous Mesoporous Mater.* 92 (2006) 270–285.
- [7] M. Selvaraj, S. Kawi, Comparison of mesoporous and microporous solid acid catalysts for highly selective synthesis of thymol by vapor phase isopropylation of m-cresol, *Microporous Mesoporous Mater.* 109 (2008) 458–469.
- [8] M. Selvaraj, D.W. Park, S. Kawi, I. Kim, Selective synthesis of benzophenone over two-dimensional mesostructured CrSBA-15, *Appl. Catal. A Gen.* 415–416 (2012) 17–21.
- [9] N.S. Nesterenko, O.A. Ponomoreva, V.V. Yuschenko, I.I. Ivanova, F. Testa, F. Di Renzo, F. Fajula, Dehydrogenation of ethylbenzene and isobutane over Ga- and Fe-containing mesoporous silicas, *Appl. Catal. A Gen.* 254 (2003) 261–272.
- [10] E. Antonakou, A. Lappas, M.H. Nilsen, A. Bouzga, M. Stöcker, Evaluation of various types of Al-MCM-41 materials as catalysts in biomass pyrolysis for the production of bio-fuels and chemicals, *Fuel* 85 (2006) 2202–2212.
- [11] M.W.E. Van den Berg, S. Polarzb, O.P. Tkachenko, K.V. Klementiev, M. Bandyopadhyay, L. Khodeir, H. Gies, M. Muhler, W. Grünert, Cu/ZnO aggregates in siliceous mesoporous matrices: development of a new model methanol synthesis catalyst, *J. Catal.* 241 (2006) 446–455.
- [12] M. Popova, Á. Szegedi, P. Németh, N. Kostova, T. Tsoncheva, Titanium modified MCM-41 as a catalyst for toluene oxidation, *Catal. Commun.* 10 (2008) 304–308.
- [13] E. Antonakou, A. Lappas, M.H. Nilsen, A. Bouzga, M. Stöcker, Evaluation of various types of Al-MCM-41 materials as catalysts in biomass pyrolysis for the production of bio-fuels and chemicals, *Fuel* 85 (2006) 2202–2212.
- [14] G.A. Eimer, S.G. Casuscelli, C.M. Chanquia, V. Elías, M.E. Crivello, E.R. Herrero, The influence of Ti-loading on the acid behavior and on the catalytic efficiency of mesoporous Ti-MCM-41 molecular sieves, *Catal. Today* 133–135 (2008) 639–646.
- [15] A. Thangaraj, R. Kumar, S. Mirajkar, P. Ratnasamy, Catalytic properties of crystalline titanium silicalites I. Synthesis and characterization of titanium-rich zeolites with MFI structure, *J. Catal.* 130 (1991) 1–8.
- [16] K.T. Li, C.C. Lin, Propylene epoxidation over Ti/MCM-41 catalysts prepared by chemical vapor deposition, *Catal. Today* 97 (2004) 257–261.
- [17] G.A. Eimer, S.G. Casuscelli, G.E. Ghione, M.E. Crivello, E.R. Herrero, Synthesis, characterization and selective oxidation properties of Ti-containing mesoporous catalysts, *Appl. Catal. A Gen.* 298 (2006) 232–242.
- [18] Y.S. Sun, X.B. Lu, S.T. Zhang, R. Zhang, X.Y. Wang, Kinetic study for Fe(NO₃)₃ catalyzed hemicellulose hydrolysis of different corn stover silages, *Bioresour. Technol.* 102 (2011) 2936–2942.
- [19] K.A. Koyano, T. Tatsumi, Synthesis of titanium-containing MCM-41, *Micropor. Mater.* 10 (1997) 259–257.